

Hydrodynamic synchronization of colloidal oscillators

Jurij Kotar^a, Marco Leoni^{a,b,c}, Bruno Bassetti^b, Marco Cosentino Lagomarsino^{b,d}, and Pietro Cicuta^{a,1}

^aCavendish Laboratory and Nanoscience Center, University of Cambridge, JJ Thomson Avenue, CB3 0HE Cambridge, United Kingdom; ^bDipartimento di Fisica and Istituto Nazionale di Fisica Nucleare, Università degli Studi di Milano, sez. Milano, Via Celoria 16, 20100 Milan, Italy; ^cDepartment of Mathematics, University of Bristol, Bristol, BS8 1TW, United Kingdom; and ^dGenomic Physics Group, FRE 3214 Centre National de la Recherche Scientifique "Microorganism Genomics" and University Pierre et Marie Curie, 15, rue de l'École de Médecine, Paris, France

Edited by Harry L. Swinney, University of Texas, Austin, TX, and approved March 16, 2010 (received for review October 28, 2009)

Two colloidal spheres are maintained in oscillation by switching the position of an optical trap when a sphere reaches a limit position, leading to oscillations that are bounded in amplitude but free in phase and period. The interaction between the oscillators is only through the hydrodynamic flow induced by their motion. We prove that in the absence of stochastic noise the antiphase dynamical state is stable, and we show how the period depends on coupling strength. Both features are observed experimentally. As the natural frequencies of the oscillators are made progressively different, the coordination is quickly lost. These results help one to understand the origin of hydrodynamic synchronization and how the dynamics can be tuned. Cilia and flagella are biological systems coupled hydrodynamically, exhibiting dramatic collective motions. We propose that weakly correlated phase fluctuations, with one of the oscillators typically precessing the other, are characteristic of hydrodynamically coupled systems in the presence of thermal noise.

colloidal particles | hydrodynamic interaction | metachronal wave | optical tweezers | nonlinear dynamical system

The self-organization of nonlinearly interacting dynamical elements into synchronized states is a "classic" topic of science, underlying a wide range of biological (1, 2) and technological processes (3). A relatively unexplored problem is the synchronization in biological flows, thought to be generated by hydrodynamic coupling at the micrometer scale. In this class of wet micron-scale problems, the coupling is mechanical but of viscous character, and the effects of thermal noise are often not negligible. Coordinated motion is crucial for the effective functioning of cilia and flagella, the elements of eukaryotic cells implicated in generating fluid flows and motility (4). Hydrodynamic coupling is also important in natural and artificial microfluidic conditions (5, 6) and low Reynolds number (Re) "microbot" swimmers (7, 8). At the relevant scales and temperatures, it has the same magnitude as the random thermal forces; nevertheless, the synchronized states of e.g. cilia are stable, so that robust mechanisms to induce them must exist. Cilia play vital roles on the surface of the respiratory tract in mammals, maintaining an upward flow of mucus, away from the lungs (9). They also determine the asymmetry of various organisms during development (10). In arrays of cilia the beating is synchronized, generating complex wave-like patterns called metachronal waves (11). Nearby sperm cells (12) also exhibit synchronized motion patterns, resulting at least in part from the interaction of neighboring oscillating flagella through the fluid (13). Recent experiments (14, 15) have explored the phenomenology of synchronized flagella in *Chlamydomonas*. Flagella and cilia are mechanically coupled by the flow of fluid, which is typically in the low Re regime (11, 16, 17).

Model

We have devised an experimental system that contains the minimal elements to probe and understand the onset of collective motion induced by hydrodynamic interaction. Two driven oscillating colloidal spheres lock into antiphase motion, showing a surprising behavior caused by the interplay of thermal noise and hydrodynamic interactions, as well as general features typical of coupled nonlinear oscillators. The "artificial model system" studied here

reduces the complexity of a biological system and can be controlled directly, enabling theoretical models to be developed and validated. Optical traps are used to confine colloidal beads within harmonic potentials (18). The bead radius is $a = 1.5 \mu\text{m}$, the trap stiffness is $\kappa = (1.55 \pm 0.07) \times 10^{-6} \text{ N/m}$, the sample viscosity $\eta = 7.4 \text{ mPa s}$ (see *SI Methods*). In the absence of other external forces, a particle in this potential undergoes overdamped stochastic motion driven by thermal forces (19). In the experiment two beads are confined in separate harmonic wells. The position of each well is linked to the spatial configuration of the beads via a "geometric switch." Specifically, the laser trap on each particle is moved between two positions a distance λ apart, as shown in Fig. 1 *A* and *B*, following the rule that the switch of trap position is triggered when a particle approaches to within a distance ξ from the minimum of the active potential. This feedback-controlled motion of the traps is sufficient to induce sustained oscillations, and each particle undergoes longtime periodic motion with amplitude $\lambda - 2\xi$, shown in Fig. 1*C*. Crucially, when more than one bead is present in the system, the geometric switch is determined independently for each bead (100 times per second), so that the external trap forces do not themselves impose the phase of oscillation nor its period.

A biological cilium is itself a complex structure; its own regular beating (and switching) is constrained by a mechanical feedback (20). In a given flow condition, the mechanical stress and the geometrical configuration are coupled parameters, and the geometric feedback condition is a simple way to account for how a cilium senses the moment to switch between so-called power and recovery strokes (11, 21). In this spirit the system investigated here can be thought of as an idealized 2-cilia experiment: The optical trap force plays the role of the molecular motors that induce active movement, and the hydrodynamic flow field produced by the moving beads well represents beating cilia, at least at large distances (17, 22). The model is also a general experimental system to probe the physics of stochastic and actively forced hydrodynamically coupled oscillators. A similar model based on a deformable rotator in place of a geometric switch has been proposed (16), tested on a macroscopic scale (23), but seems harder to realize experimentally on the colloidal scale.

The experimental system can be considered theoretically by describing the hydrodynamic interactions with the Oseen tensor \mathbf{O} (19, 24), giving the equation of motion

$$\dot{\mathbf{x}}_i = \sum_j \mathbf{O}_{ij}(\mathbf{F}_j + \mathbf{f}_j),$$
$$\text{with } \mathbf{O}_{ij} = \frac{\mathbf{I} + \hat{\mathbf{d}}_i \hat{\mathbf{d}}_j}{8\pi\eta d_{ij}} \quad \text{and} \quad \mathbf{O}_{ii} = \mathbf{I}/\gamma, \quad [1]$$

Author contributions: B.B., M.C.L., and P.C. designed research; J.K., M.L., M.C.L., and P.C. performed research; J.K., M.L., M.C.L., and P.C. analyzed data; M.C.L. and P.C. wrote the paper; and J.K. built instrumentation.

The authors declare no conflict of interest.

This article is a PNAS Direct Submission.

¹To whom correspondence should be addressed. E-mail: pc245@cam.ac.uk.

This article contains supporting information online at www.pnas.org/lookup/suppl/doi:10.1073/pnas.0912455107/-DCSupplemental.

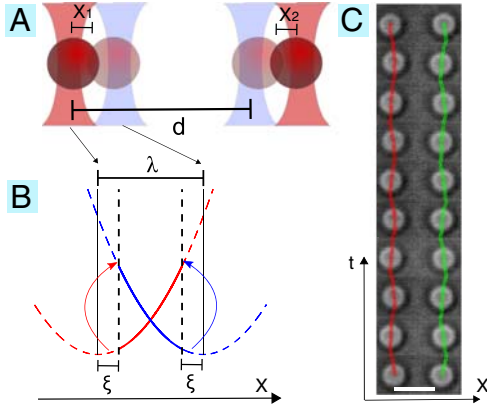


Fig. 1. The physical system. Driven oscillations of fixed amplitude, but free inphase, are obtained using optical traps. The trap alternates between two minima with a “geometric switch” triggered by the position of the colloidal particle. (A) and (B) illustrate the experimental parameters, showing the trap separation in a pair $\lambda = 1 \mu\text{m}$, the distance from the minimum at which the traps are switched $\xi = 0.248 \mu\text{m}$. The distance between trap pairs is in the range $4 \mu\text{m} \leq d \leq 40 \mu\text{m}$. (C) Two particles lock in antiphase. Particle positions overlaid on an image sequence of a pair of particles undergoing driven oscillations controlled by the geometric switch. Antiphase motion can be seen. Images are shown every 0.1 s, and data points are shown every 0.01 s. Scale bar, $5 \mu\text{m}$.

where \mathbf{F}_j is the force applied on bead j by the optical tweezers, \mathbf{f}_j is thermal noise, $\gamma = 6\pi\eta a$, $\hat{\mathbf{d}}_{ij}$ is the unit vector parallel to the vector \mathbf{d}_{ij} between beads i, j , and \mathbf{I} is the unit matrix. The thermal noise has zero mean and correlation $\langle \mathbf{f}_i(t)\mathbf{f}_j(t') \rangle = 2k_B\text{TO}_{ij}^{-1}\delta(t-t')$ in order to have equipartition (24). These equations are correct in the far field limit ($d \gg a$) and for steady flows ($d \ll \ell$, where $\ell \simeq (2\eta/(\omega\rho_f))^{1/2}$, ω is the inverse period of oscillation, and ρ_f the fluid density). The hydrodynamic interaction is thus included at the same level of approximation as in previous work (8, 19, 25), and the regime is simpler than that in ref. 26. The geometric switch is implemented as follows. Considering the displacements x_1, x_2 of the two beads about two reference positions along the x axis as in Fig. 1A (as the system has cylindrical symmetry, only the x direction is considered below), the force applied on bead i is $F_i = -\kappa(x_i + \sigma_i\lambda/2)$ where $\sigma_i \in \{-1, 1\}$ is a configuration-coupled variable that switches at the trigger positions. Formally this switch condition can be written as

$$\dot{\sigma}_i = \pm 2\delta(t - t_i^\pm), \quad [2]$$

where t_i^\pm is such that $x_i(t_i^\pm) = \pm sw$, and $sw(\sigma_i) = (\lambda/2 - \xi)\sigma_i$. As a function of time, σ_i appears as a square function, which is set by the dynamics of x_i .

The most relevant features of the model are (i) the geometric switch gives constant-amplitude but phase-compliant oscillations and thus the generic possibility to synchronize; (ii) the inverse bead separation sets the coupling strength, which interplays with thermal noise (this effect is also related to the trap stiffness); (iii) there is a characteristic beating time of the single oscillators, given by their typical arrival time at the switch, which can be set to be the same or different for the two beads.

We have realized the system experimentally and solved numerically Eqs. 1 and 2 using the method of Ermak and McCammon (27). Eq. 1 can be linearized ($d_{ij} \simeq d$) if the oscillations are small ($\lambda \ll d$) (19). Numerical simulations show that under the experimental range of conditions this linearization does not influence the numerical results. We have solved the linearized equations in absence of noise, piecewise between each switch event, and obtained a deterministic solution in the form of a map as shown in *SI Discussion*. Finally, we have considered the linearized equations with noise to provide analytical arguments supporting our experimental and numerical observations.

Results

Oscillators Lock into Antiphase. We first briefly discuss the analytical solution with no noise, which is useful for the interpretation of the results discussed later (see also *SI Discussion* for more details). The general solution of the equation of motion Eq. 1 is $x_\pm(t) = x_\pm(0) \exp(-t/\tau_\pm)$, where $x_\pm = x_2 \pm x_1$ and x_1, x_2 are the displacements of the two beads about their reference positions, and $\tau_\pm = \tau_0(1 \pm 3a/2d)^{-1}$ ($\epsilon = 3a/2d$ quantifies the strength of the hydrodynamic coupling).

Starting from an arbitrary initial condition, this solution can be propagated until one particle reaches the switch. At this point, the same solution remains valid, changing one potential and setting the initial condition as the switch point. Iterating this procedure leads to a map from the space of initial conditions. The only fixed points are the antiphase and the inphase state. Stability analysis shows that only the antiphase state is stable. Furthermore, the relaxation dynamics towards the stable state can be calculated: a perturbation $h = 1 - r/\rho$ from the antiphase state, i.e. from the configuration where particle 1 has displacement $x_1(0) = -\rho$ and particle 2 has position $x_2(0) = r < \rho$, where $\rho = \lambda - \xi$, is damped following the equation $\dot{h} = -\epsilon B h$, where the dot indicates a derivative with respect to time in cycles, B is a geometric parameter depending on the positions ρ and ξ of the switch points, and ϵ quantifies the coupling strength. Since h can be interpreted as a “phase difference” with respect to a stable antiphase state, this phenomenology is similar to other models for cilia or general oscillators (3, 16, 23).

Thus, the deterministic equations of motion have a single stable analytic solution, with the beads oscillating exactly in antiphase. In the absence of noise, an isolated particle would oscillate with a period $P = 2\tau_0 \log((\lambda - \xi)/\lambda)$, where τ_0 is the relaxation time in a harmonic potential, determined by $\tau_0 = \gamma/\kappa$. With two particles interacting through the hydrodynamic flow in the viscous solvent the hydrodynamic coupling is sufficient to induce the synchronization of the two oscillators. Other possible interactions (electrostatic, dispersion forces, trap cross-talk) are negligible for the interparticle distances studied here. The resulting motion is, to a first approximation, in antiphase. Fig. 2A shows typical trajectories.

Fig. 2B shows the power spectrum of bead displacement during the experiment, with the deterministic solution describing well the experimental result of synchronization and the dependence of the locking frequency on the distance between beads: Fig. 2C shows that as d is reduced, the drag increases and the power spectrum shifts to lower frequencies. The inphase (+) and antiphase (−) modes are decoupled (19) and have the relaxation times τ_\pm given above. The deterministic relaxation time is $\tau_{\text{det}} = \tau_- \log(\rho/\xi)$ for the antiphase mode. The frequency of bead motion in coupled oscillations in the absence of noise is therefore $\omega_{\text{sync}} = 1/(2\tau_{\text{det}})$, in good agreement with the data of Fig. 2C.

The phase correlation between beads is quantified by calculating the order parameter:

$$Q(t) = - \frac{\int_t^{t+6\tau} x_1(t')x_2(t')dt'}{\sqrt{\int_t^{t+6\tau} x_1^2(t')dt' \int_t^{t+6\tau} x_2^2(t')dt'}} \quad [3]$$

where the moving time window spans three periods ($\simeq 110$ frames). Q is constructed so that $Q = 0$ for uncorrelated signals, $Q = 1$ for antiphase motions, and $Q = -1$ for inphase (see *SI Text*, Fig. S1 and Table S1). The distribution of $Q(t)$ over an entire experiment is presented in Fig. 3A, for different values of bead separation. The initial conditions (in both experiment and numerical simulation) are irrelevant; the runs are started inphase, but after at most a couple of cycles the beads are either antiphase or at random phase difference. In Fig. 3C the distribution of $Q(t)$ is plotted for different stiffness ratios of traps 1 and 2: κ_1/κ_2 . The antiphase

correlation is strongest for the largest coupling parameter ($1/d$), i.e. minimum d , and for equal trap stiffness.

Synchronization is Lost by Increasing Noise or Detuning the Oscillators.

As may be expected, the thermal noise can lead to loss of synchronization. This is seen clearly when the coupling strength is reduced by increasing the distance between the particles, Fig. 3 A and B. This is one of the factors that determine $Q < 1$ even at the maximum coupling. As the coupling parameter is reduced, the arrival times of the beads at the switch positions are increasingly stochastically different. Two effects are observed which contribute to the loss of synchronization: “phase-slipping” and “drowning” in noise. The phase-difference of the two oscillators may exhibit an increasing number of steps, visible in Fig. 3 B for intermediate coupling strength. The steps are “phase-slips” (3) or barrier hopping events. The standard deviation of arrival times, evaluated in between slip events, is shown in the bottom panel of Fig. 3 B. This random time difference grows with noise, up to the half-period $P/2$ when the loss of synchronization is complete, and the phase-difference plot shows a random drift. The loss of synchronization process can be followed in the progressive broadening of the distribution of Q towards $Q = 0$ as coupling is weakened, resembling a second order phase transition.

In general, for weakly coupled stochastic oscillators to synchronize, the intrinsic frequencies must be nearly equal (3). Fig. 3C shows synchronization of oscillators with different frequencies, provided that the intrinsic frequencies are close. In these experiments, the stiffness of the two traps is set to different values, which changes the decay rate τ_0 for each bead. This can be thought of as detuning the oscillators. The resulting behavior is shown experimentally for $d = 10 \mu\text{m}$ and is calculated numerically for a range of d (additional data are shown in Fig. S2). Fig. 3C shows that the region of trap strength ratio in which synchronization occurs vanishes as the distance increases, i.e. as the coupling becomes weaker. Many models showing synchronization display similar trends, with the synchronization region delimited by approximately linear boundaries (3). In the loss of synchronization due to detuning, the phase slips and the drift are not random, but biased, thus this system is comparable to a random walker in a tilted periodic potential (28). Inspection of the deterministic version of the geometric switch model (see SI Discussion) indicates that a weak detuning of the intrinsic frequencies results in a linear perturbation of the antiphase fixed point, similarly to other models for cilia synchronization described in the literature (16).

Discussion

Noise and Hydrodynamic Interactions Cause a Stochastic Delay Time.

Surprisingly, the main reason for never observing perfect synchronization ($Q < 1$ in Fig. 3A) is that there is a stochastic but typically finite delay in the motion of the coupled beads. This element is especially interesting because it is specific of synchronization due to hydrodynamic interactions in a Brownian system. The relative phase of the two oscillators has small fluctuations from cycle to cycle. Within each time window of the experimental series, the delay time Δt is measured by finding the maximum value of anticorrelation as the lag time is varied. This time Δt represents the shift of the two oscillators, relative to the antiphase state, and can be positive or negative. Δt has zero mean and its time autocorrelation function decays exponentially with a timescale of a few half periods, depending on the coupling strength, Fig. S3. This decay time can be understood theoretically by an analysis of the stability of a perturbed antiphase locked state (details in SI Discussion). However, $|\Delta t|$ is typically finite. Fig. 4A shows the distribution of the absolute value $|\Delta t|$, which has peaks at finite values of switch time difference. These peaks at finite delay time are most evident as the coupling strength increases. The measured time interval is up to 5-fold larger than the experimental feedback time, thus $|\Delta t|$ is not simply an effect of having to wait a feedback

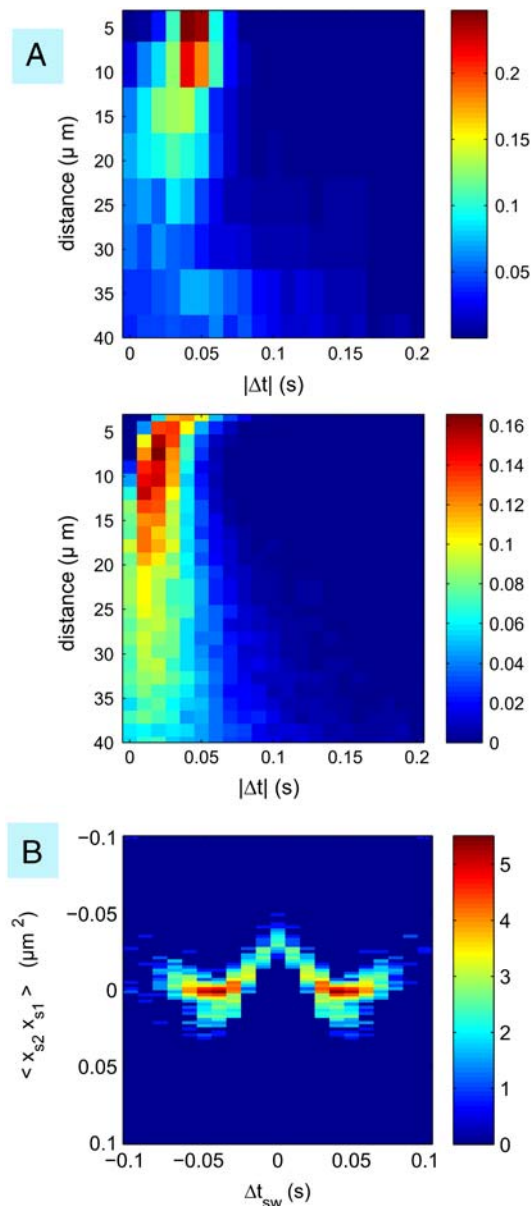


Fig. 4. The fingerprint of hydrodynamic synchronization. In the presence of thermal noise, a characteristic delay time emerges between subsequent switches. The bead oscillations are delayed by a finite time Δt . (A) Heatmap for the distribution of $|\Delta t|$ at varying distance, measured in the experiment (Top) and by numerical simulation (Middle), shows the peak value of $|\Delta t| \rightarrow 0$ and also a broadening of the distribution with increasing d . (B) Heatmap of the cross-correlation of switch positions as a function of the delay time, showing strong correlation at finite time intervals.

delay time to enable the trap switch. A proof of this is also obtained by simulating the system with varying feedback times. The experimental feedback time is an irrelevant parameter in relation to this effect (see SI Methods and Figs. S4 and S5).

To understand the origin of this typical delay, a simpler scenario can be considered. Two trapped beads, at distance d apart, are released from opposite displacements. The statistics of the time difference in reaching a limiting displacement $\pm \xi$ are collected. Trap switches are absent. A similar phenomenology of finite Δt is already present here (see SI Text and Figs. S6, S7, and S8). This result indicates that the presence of a delay is a fundamental feature of a family of problems and is most likely originating from the correlation of first passage times of two hydrodynamically coupled beads, for which unfortunately we have no analytical

expression. This effect is related to previous observations (19, 29) that a system composed of two beads in a pair of stationary traps undergo fluctuations which are anticorrelated with a stochastic delay of about τ_0 . However, through the geometrical switch the correlation of fluctuations becomes a global feature of the beating of the oscillators. The correlation between switch times is also reflected in a correlation of the switch positions. Fig. 4B shows that the position x_{s1} of the first bead at the moment the second bead switches is correlated with the position x_{s2} of the second bead when the first bead switches. This correlation depends on the time interval between the switch events, and the most striking result is that the maximum of correlation occurs for finite switch time intervals.

To conclude, this work shows clearly that thermal noise sets an upper cutoff on the distance between oscillators to sustain synchronization in low viscosity liquids. The cutoff distance will depend on system parameters, in particular the beating frequency and the viscosity; in the conditions studied here synchronization is lost beyond 40 μm . Effects that arise from changes in the beat frequency have been shown, and some biological systems might benefit from these. For example in *Chlamydomonas* there is a synchrony loss when the sudden change of the intrinsic frequency of one of the two flagella causes detuning (14). This leads to swimming trajectories with sharp turns, analogous to the run-and-tumble mechanism used by bacteria (30). Our system can be used to

gain more insight into this phenomenon, which would also be relevant in artificial swimmers (7, 8). The model studied here can stabilize inphase motion with slight variations (21) and we expect this to be relevant in determining the conditions necessary to obtain *inphase* synchronization. In *Chlamydomonas*, for example, both “breast-stroke” and inphase wave-like motion are observed. In previous theoretical work (21) we showed that extended linear chains of geometrical-switch active oscillators can sustain propagating waves.

A general question that this system can help answer is whether the source of synchronization observed in cilia and flagella is actually of hydrodynamic origin. At the moment this is a speculation consistent with a number of experimental observations (9, 11, 15, 21). The characteristic delay time we have found should not be generally present in stochastic synchronizing systems where the coupling does not induce the same correlation properties in the noise (31). Thus, with further investigation, it might be shown to be a useful “fingerprint” of the hydrodynamic origin of flagellar synchronization.

ACKNOWLEDGMENTS. We are grateful to A. Gamba, G. Boffetta, D. Frenkel, M. E. Cates, R. Goldstein, F. De Lillo, N. Kern, M. Polin, and I. Tuval for very useful discussions. We acknowledge funding from Engineering and Physical Sciences Research Council and the Royal Society.

- Winfrey A (1967) Biological rhythms and the behavior of populations of coupled oscillators. *J Theor Biol* 16:15–42.
- Walleczek J (2000) *Self-Organized Biological Dynamics & Nonlinear Control* (Cambridge Univ Press, New York).
- Pikovsky A, Rosenblum M, Kurths J (2001) *Synchronization* (Cambridge Univ Press, Cambridge, U.K.).
- Bray D (2000) *Cell Movements: From Molecules to Motility* (Garland Science, New York).
- Beatus T, Tlustý T, Bar-Ziv R (2006) Phonons in a one-dimensional microfluidic crystal. *Nat Phys* 2:743–748.
- Hänggi P, Marchesoni F (2009) Artificial brownian motors: Controlling transport on the nanoscale. *Rev Mod Phys* 81:387–441.
- Putz VB, Yeomans JM (2009) Hydrodynamic synchronization of model microswimmers. arXiv:0907.1542v1.
- Leoni M, Kotar J, Bassetti B, Cicuta P, Cosentino Lagomarsino M (2009) A basic swimmer at low Reynolds number. *Soft Matter* 5:472–476.
- Gheber L, Priel Z (1994) Metachronal activity of cultured mucociliary epithelium under normal and stimulated conditions. *Cell Motil Cytoskeleton* 28:333–345.
- Cartwright JHE, Piro N, Piro O, Tuval I (2008) Fluid dynamics of nodal flow and left-right patterning in development. *Dev Dynam* 237:3477–3490.
- Gueron S, Levit-Gurevich K, Liron N, Blum J (1997) Cilia internal mechanism and metachronal coordination as the result of hydrodynamical coupling. *Proc Natl Acad Sci USA* 94:6001–6006.
- Taylor GI (1951) Analysis of the swimming of microscopic organisms. *P R Soc London* 209:447–461.
- Fauci LJ, McDonald A (1995) Sperm motility in the presence of boundaries. *Bull Math Biol* 57:679–699.
- Polin M, Tuval I, Drescher K, Gollub JP, Goldstein RE (2009) *Chlamydomonas* swims with two “gears” in a eukaryotic version of run-and-tumble locomotion. *Science* 325:487–490.
- Goldstein RE, Polin M, Tuval I (2009) Noise and synchronization in pairs of beating eukaryotic flagella. *Phys Rev Lett* 103:168103.
- Niedermayer T, Eckhardt B, Lenz P (2008) Synchronization, phase locking, and metachronal wave formation in ciliary chains. *Chaos* 18:037128.
- Lauga E, Powers TR (2009) The hydrodynamics of swimming microorganisms. *Rep Prog Phys* 72:096601.
- Block S (1992) Making light work with optical tweezers. *Nature* 360:493–495.
- Meiners JC, Quake SR (1999) Direct measurement of hydrodynamic cross correlations between two particles in an external potential. *Phys Rev Lett* 82:2211–2214.
- Hilfinger A, Chattopadhyay AK, Jülicher F (2009) Nonlinear dynamics of cilia and flagella. *Phys Rev E* 79:051918.
- Cosentino Lagomarsino M, Jona P, Bassetti B (2003) Metachronal waves for deterministic switching two-state oscillators with hydrodynamic interaction. *Phys Rev E* 68:021908.
- Brennen C, Winet H (1977) Fluid mechanics of propulsion by cilia and flagella. *Annu Rev Fluid Mech* 9:339–398.
- Qian B, Jiang H, Gagnon DA, Breuer KS, Powers TR (2009) Minimal model for hydrodynamic synchronization. arXiv:0904.2347v2.
- Doi M, Edwards SF (1986) *The Theory of Polymer Dynamics* (Oxford Univ Press, New York).
- Polin M, Grier D, Quake S (2006) Anomalous vibrational dispersion in holographically trapped colloidal arrays. *Phys Rev Lett* 96:088101.
- Liverpool TB, MacKintosh F (2005) Inertial effects in the response of viscous and viscoelastic fluids. *Phys Rev Lett* 95:208303.
- Ermak DL, McCammon JA (1978) Brownian dynamics with hydrodynamic interactions. *J Chem Phys* 69:1352–1360.
- Reimann P, et al. (2002) Diffusion in tilted periodic potentials: Enhancement, universality, and scaling. *Phys Rev E* 65:031104.
- Hough LA, Ou-Yang HD (2002) Correlated motions of two hydrodynamically coupled particles confined in separate quadratic potential wells. *Phys Rev E* 65:021906.
- Berg HC, Brown DA (1972) Chemotaxis in *Escherichia coli* analyzed by three-dimensional tracking. *Nature* 239:500–504.
- Freund J, Schimansky-Geier L, Hänggi P (2003) Frequency and phase synchronization in stochastic systems. *Chaos* 13:225–238.